Characterization of Shallow Soil Profiles Using Geophysical Tests

Paul Groves
Giovanni Cascante, P.Eng., Ph.D.
Department of Civil Engineering – University of Waterloo, Waterloo, Ontario, Canada
Dave Dundas, P.Eng.
Ministry of Transportation Ontario, Toronto, Ontario, Canada
P.K. Chatterji, P.Eng., Ph.D.
Thurber Engineering Ltd., Oakville, Ontario, Canada

ABSTRACT
An investigation was performed to evaluate the applicability of specific geophysical methods for geotechnical site characterization in environmentally sensitive wetland areas. Three geophysical methods were explored: electrical resistivity imaging, seismic refraction, and multiple-channel analysis of surface waves. On-site boreholes revealed three softer layers overlying a stiffer till. The complementary use of geophysical techniques was successful in determining the stratigraphy and the depth of the competent layer (till) at the test site. The results indicate these methods have the potential to improve subsurface model accuracy and reduce the number of boreholes for investigations in sensitive zones.

RÉSUMÉ
Une investigation a été effectuée pour évaluer l'applicabilité de certaines techniques géophysiques pour la charactérisation géotechnique des zones environnementalement sensibles. Trois méthodes géophysiques ont été adoptées: l'imagerie resistivitée électrique, la refraction sismique, et l'analyse multi-canals des ondes de surface. Les échantillons prélevés sur le site ont révélé la presence de trois strates meubles recouvrant une strate de till glaciaire plus compacte. L'utilisation complémentaire de ces méthodes géophysiques s'est avérée concluante pour identifier la stratigraphie et la profondeur du till glaciaire sur le terrain. Les résultats indiquent que ces méthodes ont le potentiel de réduire le nombre de forages pour les investigations dans les zones sensibles.

1 INTRODUCTION

The design and construction of foundation projects require information about the engineering properties and extents of the subsurface soils. An important aspect of foundation investigations is the identification of a competent layer and its depth. Conventional site characterization involves the drilling of boreholes at widely separated locations to generate a profile of soil layers. The drilling of a sufficient number of boreholes to adequately establish a subsurface model is often constrained by factors such as available budget, access of drilling equipment to difficult terrain, environmental regulations, and permissions to enter properties.

In light of the above constraints, selected geophysical techniques were investigated to assess if they would provide sufficient information, when supported by a limited number of complimentary boreholes, to delineate stratigraphy. Geophysical methods can be conducted at the ground surface and thus are non-intrusive, relatively inexpensive, fast, and environmentally friendly techniques for interpreting stratigraphy by measuring the change in geophysical properties of different soil layers. The accuracy and resolution of these techniques have improved significantly in recent years due to advances in equipment and data processing.

This paper presents field results from geophysical investigations performed to evaluate their applicability for geotechnical site characterization. The investigations consisted of testing three selected geohphysical methods across two 188 m lines and verifying the results by drilling boreholes. The geophysical methods tested were electrical resistivity imaging (ERI), seismic refraction (SR), and multiple-channel analysis of surface waves (MASW). The trial site is located in an environmentally sensitive wetland area along a proposed highway extension corridor. Previous studies for the area suggested the presence of very soft compressible soils underlain by hard glacial till.

2 THEORETICAL BACKGROUND

2.1 Electrical Resistivity Imaging (ERI)

The ERI method measures the resistivity (Ohm-metre, Ω-m) or its reciprocal, electrical conductivity (Siemens/metre, S/m), of the tested medium. It is common practice to plot the conductivity of the medium instead of the resistivity because it is better correlated with the stratigraphy of the medium.

A resistivity test involves many measurements. Each measurement involves four electrodes. Two electrodes introduce current flow (I) into the ground. Two additional electrodes, located in different locations, simultaneously measure the electrical potential changes (ΔV) in the ground due to the imposed current flow (Figure 1).

The resistivity (ρ) of the soil between the potential

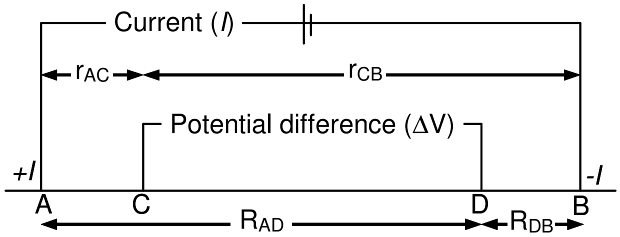

Figure 1. General electrode configuration for ERI

measuring electrodes is computed as (Keary et al. 2002)

$$\rho = \frac{2\pi\Delta V}{I\left\{\left(\frac{1}{r_{AC}} - \frac{1}{r_{CB}}\right) - \left(\frac{1}{R_{AD}} - \frac{1}{R_{DB}}\right)\right\}} \quad [1]$$

where r_{AC}, r_{CB}, R_{AD}, and R_{DB} are the relative positions of the electrodes (Figure 1).

The spacing of the electrodes is changed to generate a resistivity profile. The increase of electrode spacing increases the effective depth of penetration. Inversion software is used to generate a two-dimensional electrical resistivity structure of the ground below the survey line.

The ERI survey can give some indication of lithology, especially when used in conjunction with other information such as borehole logs. It is difficult to determine lithology from resistivity surveys alone because the electrical resistivity/conductivity is affected by several factors at the same time (e.g. porosity, degree of saturation, concentration of dissolved electrolytes in the pore water, temperature and phase state of the water in the pore spaces, and the amount of clay minerals and colloidal material) (McNeill 1980).

2.2 Seismic Refraction (SR)

The SR method measures the velocity of seismic body waves (compressional waves, p-waves, or shear waves, s-waves) as they are refracted from different layers in the subsurface. The transmission velocities of p-waves (V_p) and s-waves (V_s) through a homogeneous material are given by

$$V_P = \sqrt{\frac{B + \frac{4}{3}G}{\rho}} \quad [2]$$

$$V_S = \sqrt{\frac{G}{\rho}} \quad [3]$$

where B is the bulk modulus, G is the shear modulus, and ρ is the mass density of the medium.

A refraction survey requires an array of equally spaced geophones, which measure vertical or horizontal motion, and a seismic source, such as a sledgehammer, weight drop, or explosive charge. Seismic traces (velocity versus time) are collected from the geophone array at several source locations along the line.

SR surveys analyze the first arrival event to each geophone of the array. Figure 2 illustrates a general geophone array setup for a two-layer medium (low velocity layer, V_1, over a higher velocity half-space, V_2). For the geophones located closest to the source, the first arrival event is usually the direct wave from the source. This direct wave propagates entirely in the upper medium and is a measure of the wave velocity of the near surface medium.

There is a critical distance from the source beyond which body waves that are refracted along the interface between the layers arrive before the direct wave. The first arrivals at greater distances from the source correspond therefore to the refracted waves. A plot of first arrival 'times versus distance' for a two-layer medium shows two linear events (Figure 2). A multi-layered medium would show a linear event for each layer as long as the velocity of each respective layer increases with depth.

Once the layer velocities have been established for the simple two-layer case, the depth to the refracting boundary (z) can be determined according to (Keary et al. 2002)

$$z = \frac{T_i V_1 V_2}{2(V_2^2 - V_1^2)^{1/2}} \quad [4]$$

where T_i is the intercept time (Figure 2)

Different SR interpretation techniques, such as the plus-minus method (Hagedoorn 1959) and the. generalized reciprocal method (Palmer 1981), have been

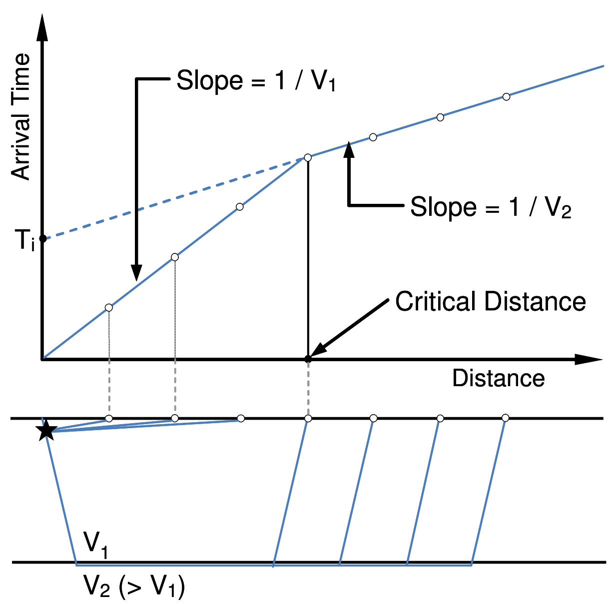

Figure 2. General case for SR

developed to determine the medium velocities and depths of different layers even if the interfaces are irregular. In addition, the ray tracing modelling technique (Cerveny et al. 1974) can be used to account for horizontal and vertical velocity gradients within the layers.

One of the limitations of the seismic refraction survey is the inability to resolve inverse layering (wave velocity decreasing with depth) which is present in the case studied.

2.3 Multiple-Channel Analysis of Surface Waves (MASW)

The MASW method uses the dispersive nature of surface waves to obtain an interpretation of multi-layered systems. When a seismic pulse is created on the ground surface most of the seismic energy travels in the form of surface waves (Rayleigh waves). In the presence of different soil layers the surface wave velocity depends not only on the properties of the medium but also on the frequency content of the excitation (Graff 1991). The depth of penetration into the medium is a function of wavelength with longer wavelengths penetrating deeper into the medium (Figure 3). The effective depth of penetration of a surface wave is commonly taken as 1/3 the wavelength. High frequencies (short wavelengths) propagate at the velocity of the first layer; whereas low frequencies (large wavelengths) propagate at a velocity determined by the characteristics of different layers (Lai and Wilmanski 2005).

The velocity of surface waves (V_R) in a homogeneous medium can be approximated as a function of V_s and the Poisson's ratio (ν) of the material by (Santamarina et al. 2005)

$$V_R \approx \frac{0.874 + 1.117\nu}{1+\nu} V_S \quad [5]$$

For ν ranging from 0 to 0.5, equation 5 indicates that V_R is approximately 0.87 to 0.96 of V_S. Consequently, Rayleigh waves can be used to estimate the shear velocity profile of a medium.

The MASW method, as the SR method, utilizes an array of geophones and a seismic source. The entire length of the time traces is analyzed versus only the first arrival times as in SR interpretation. The change in phase ($\Delta\phi$) between geophones for different frequency components of the signal are measured. The measured $\Delta\phi$ along with the geophone spacing (Δx) are used to calculate the phase velocity (V_{ph}) at a given frequency (f) according to

$$V_{ph}(f) = 2\pi f \frac{\Delta x}{\Delta\phi(f)} \quad [6]$$

The calculated V_{ph} is an average velocity of the medium between two receivers. A dispersion curve is generated by plotting the variation in phase velocity with frequency; this curve shows how different frequencies penetrating to different depths propagate at different velocities through the layered medium. A dispersion curve can be inverted, through specialized software packages, to provide the shear velocity profile of a medium. Although velocity reversals make interpretation of MASW data more difficult, they can be identified and compensated for.

The inherent problem of the MASW method is the difficulty of generating low frequencies to reach greater penetration depths with adequate signal-to-noise ratio (Stokoe et al. 1988).

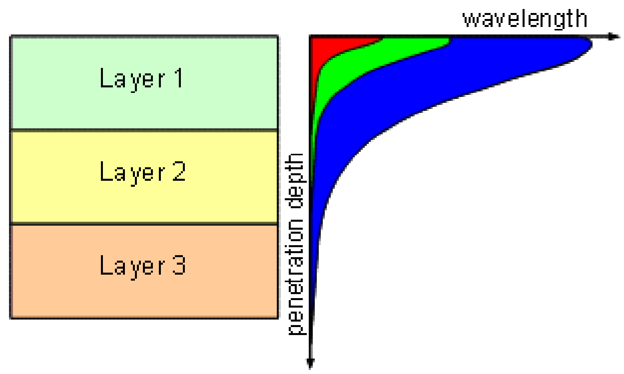

Figure 3. Wavelength effect on penetration depth of surface waves

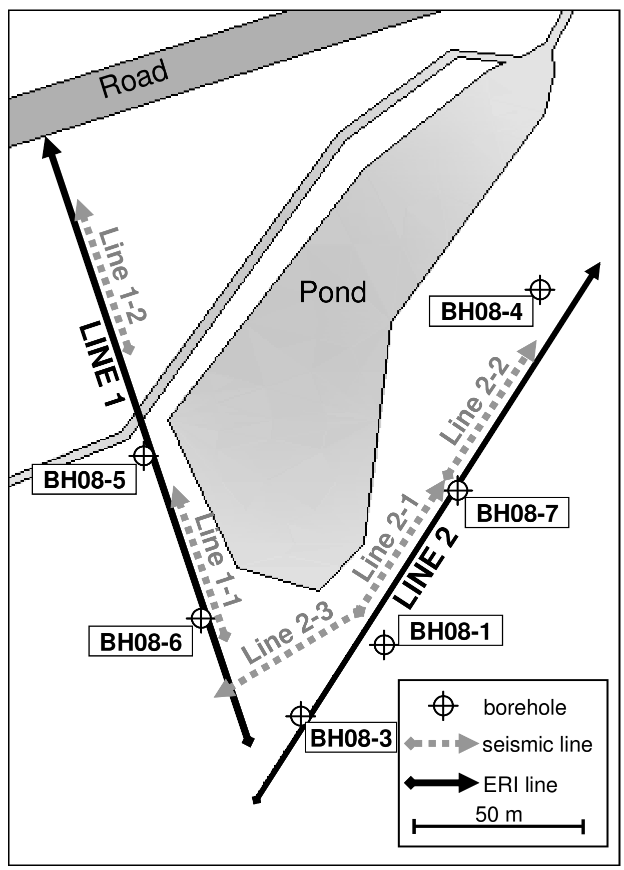

Figure 4. Survey line and borehole locations

3 GENERAL METHODOLOGY

This study involved field measurements along two 188 m lines. Line 1 ran from almost south to north, passing west of a pond and ending near a road (Figure 4). Line 2 ran from southwest to northeast along the southeast side of the pond. The ERI measurements were conducted first along the full 188 m of each line.

The seismic surveys (SR and then MASW) were subsequently completed along five 47-metre lines: two lines along Line 1 (Lines 1-1 and 1-2) and three lines along Line 2 (Lines 2-1 through 2-3) (Figure 4). The shorter line span was dictated by the geophone spacing necessary for the required depth resolution. These survey lines required 20 m clearance at each end for placement of the seismic source (170-pound weight drop). A stream to the northwest of the pond interrupted Line 1; as a result only two seismic survey lines were completed along Line 1. Thick forest along the south border of the site required the deviation of Line 2-3 alignment from Line 2.

Finally, five boreholes were advanced following the geophysical investigation (Figure 4). No drilling was completed along Line 1-2 because it was located between two residences. BH08-01 was completed prior to the geophysical surveys.

4 EXPERIMENTAL SETUP AND PROCEDURE

4.1 ERI

A 48-electrode system was used for the resistivity measurements (Syscal Junior Switch). The electrodes were driven 20 cm into the ground in a straight line at 4 m spacing for both lines. The resistivity meter was positioned at the centre of the line. The two lines were surveyed using the Wenner electrode array (equal spacing between electrodes). In addition to the two main lines, a higher resolution survey with a 2 m electrode spacing was performed from 48 m to 142 m on Line 2. This shorter survey (94 m long) gave a shallower and more detailed indication of the resistivity structure over the middle part of Line 2.

The system automatically performed a series of electrical resistivity measurements using different electrode locations and different electrode spacings. With this system, changing electrode locations corresponds to changing the lateral location of the measurement.

4.2 SR

The seismic refraction survey was performed using a 48-channel seismograph (Geode seismic recorder) and 50 Hz horizontal geophones. The geophone spacing was 1 m for a total spread length of 47 metres. Approximately 10 cm of top soil was removed at the locations of the geophones and the seismic source to enhance the coupling of the transducers with the ground. Good coupling is required to increase the signal-to-noise ratio.

The seismic source was a 25-pound sledgehammer. S-waves were generated by hitting a c-shaped steel plate in the direction perpendicular to the geophone line. S-waves were used because of their smaller wavelength and therefore better resolution in comparison with p-waves. The edges of the c-plate were partially inserted into the ground to enhance the coupling between the plate and the ground.

Seismic traces were collected for source offsets of 0.5 m, 10 m, and 20 m at the left and right hand sides of the geophone array, and one shot at the centre of the array. The source offsets were selected in the field so that sufficient refractions from the shallow and deep layers were obtained. The farthest offset shots for Line 1-2 were placed at 18 m because of the interference of a road at the north end of Line 1 (Figure 4). For each source location, positive and negative polarity shear waves were generated by hitting the steel plate in opposite directions. The change in wave polarity is used to enhance the interpretation of the first arrival times because any generated p-waves do not change polarity. Five blows on either side of the plate were recorded and stacked to improve the signal-to-noise ratio.

4.3 MASW

The MASW data was collected at the same locations and using similar equipment as the seismic refraction data. Three source offsets were chosen (2 m, 6 m, and 20 m) on either side of the lines. The shorter offset is used to study the propagation of high frequencies (shallower layers); whereas the larger offset is used to study the propagation of low frequencies (deeper layers).

The surface wave surveys were performed using the same 48-channel seismograph (Geode seismic recorder) with low-frequency 4.5 Hz vertical geophones. The geophone spacing was 1 m for a total spread length of 47 metres. The top 10 cm of soil was removed from the selected source locations and geophone locations to enhance the coupling with the ground. Different seismic sources were tested in a preliminary on-site investigation to select the best source for generating lower frequencies. The most effective seismic source was a 170-pound weight raised and dropped onto a steel plate using a tripod-pulley system.

5 RESULTS AND DISCUSSION

5.1 ERI

The depths to the competent till layer predicted by the resistivity survey and their comparison with the borehole data are presented in Table 1. A typical cross-section generated from the ERI inversion is shown in Figure 5. Inversion of the ERI data was completed using commercial software (Res2dinv, ver. 3.55, Geotomo Software 2006). The resulting cross-sections for Lines 1 and 2 generally show two obvious layers: a high conductivity layer (7.6 to 13.5 mS/m) overlying a lower conductivity layer (2 to 4 mS/m). The simplest lithological system that is consistent with these results is an upper clay rich layer and a lower layer containing more sands, silts and gravels. The less conductive material was taken to represent the till.

Table 1 indicates a range of -2.5 m to +1.3 m between

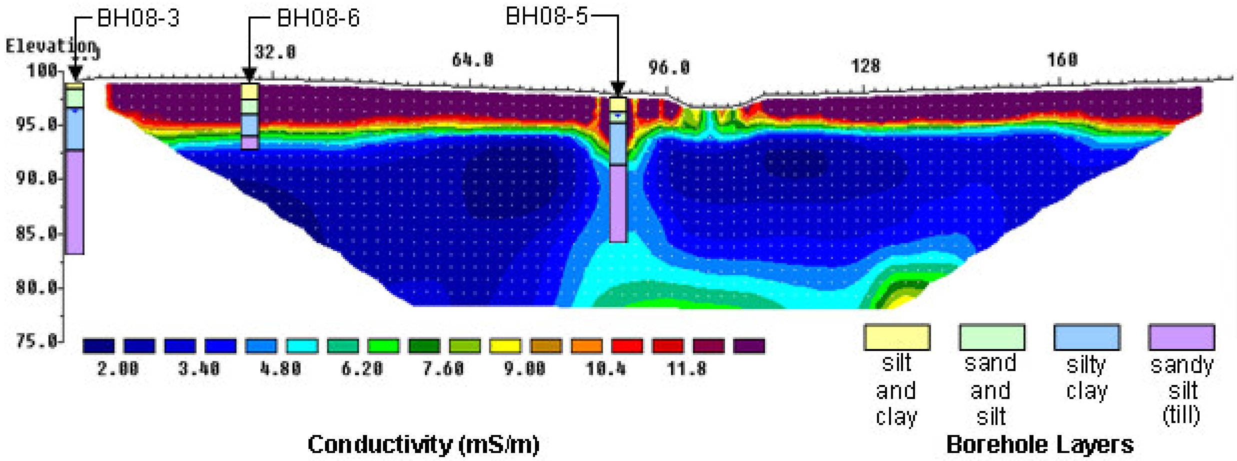

Figure 5. Typical ERI profile (Line 1 - 4 m electrode spacing)

the depths of the till obtained through the ERI analysis and the borehole measurements. The maximum error (-2.5 m) occurred at BH08-01, which was drilled prior to the geophysical survey and is located approximately 8 m offset from Line 2 (Figure 4). The next highest error (+1.3 m) occurred at BH08-4 which is located approximately 10 m offset from Line 2 (Figure 4). In addition, the location of this hole is approximately 15 m before the end of Line 2 whereas the inversion algorithm only provides results for the depth of the till in Line 2 beginning at approximately 20 m from the ends of the line. The till boundary is outside the scope of the ERI inversion at BH08-04. The depth of the till from the ERI data used in the comparison was extrapolated from the downward slope observed in the boundary near the end of the line. Except for the errors introduced by the locations of these two boreholes, the ERI measured depths to till show very good agreement with the borehole data.

The boreholes revealed three general layers overlying the till. The resolution of the ERI surveys with 4 m electrode spacing was not sufficient to accurately locate these upper lithologies. The 4 m spacing survey of Line 1 indicated only one layer overlying the till with a conductivity range of 12.5 to 13.5 mS/m (Figure 5). This inversion accurately detected what appeared to be a pre-existing channel of the on-site stream which correlated well with the depth-to-till from BH08-5. A decrease in the conductivity in the upper layer below the existing stream is also observed in the ERI inversion for Line 1. This trend is consistent with the phenomenon of fresh water in proximity to the stream being more resistive than pore water further from the stream.

Table 1. Depth of till predicted by ERI

	Depth to Hard Till (m)		
BH No.	From BH	From ERI	Difference
08-1	9.0	6.5	-2.5
08-3	6.1	6.3	0.2
08-4	10.7	12	1.3
08-5	6.1	5.7	-0.4
08-6	4.6	4.8	0.2
08-7	10.1	9.9	-0.2

The profile from the 4 m spacing survey of Line 2 identified two layers above the till layer, although the second layer was most prominent within the second half of the line. The upper-most less conductive layer (7.6 to 9.7 mS/m) identified in the inversion is consistent with the sand and silt layer identified in the boreholes. The more conductive layer (10.4 to 13.2 mS/m) overlying the till is consistent with the soft clay layer identified in the boreholes.

The ERI survey with 2 m electrode spacing completed along the middle interval of Line 2 clearly identified three layers above the till that matched the data from BH08-7; an upper layer of higher conductivity (10.4 to 13.2 mS/m) consistent with the surficial silt and clay layer, a second layer of lesser conductivity (7.6 to 9.7 mS/m) consistent with the sand layer, and finally a third layer overlying the till of higher conductivity (10.4 to 13.2 mS/m) consistent with the clay layer identified in the boreholes. However, the 2 m spacing ERI survey had less resolution at depth and underestimated the depth of the till by approximately 2.0 m.

5.2 SR

A typical velocity profile generated from the refraction analysis is presented in Figure 6. The reciprocal method analyses for the five survey lines showed only two refracting boundaries across the site; a slower refracting boundary with shear wave velocity ranging from 300 m/s to 500 m/s overlying a faster refracting boundary with a shear wave velocity ranging from 723 m/s to 928 m/s. These values are in the range of expected velocities for the materials identified by the boreholes. The upper refractor was taken as the contact between the surficial silt and clay layer and the underlying, more competent

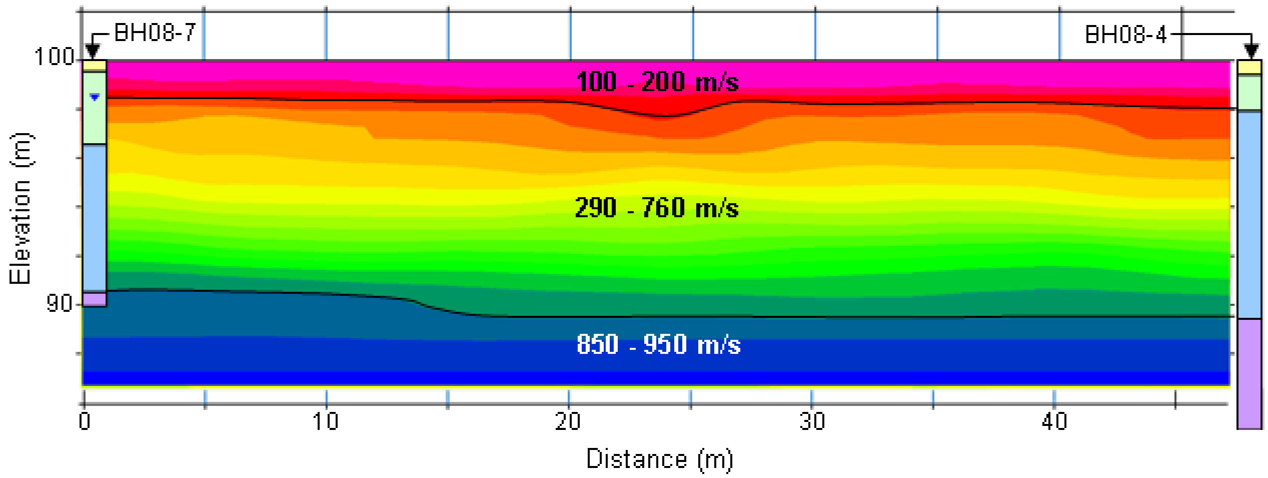

Figure 6. Typical refraction velocity profile (Line 2-2)

(and thus higher velocity) sand and silt layer. The lower refractor was taken as the upper boundary of the till. An intermediary refracting boundary (between the second and third layers from the surface) was not detected because of the inverse layering identified across the site in the borehole investigation. The second layer from the surface, composed of relatively competent sand and silt, is underlain by a softer silty clay layer, resulting in a velocity inversion from which energy is not refracted upwards.

Tomographic inversions (ray tracing method, Menke 1999) were then completed for each line using commercial software (Seisimager/2D, ver. 3.1, Geometrics 2005) by inputting the velocities and approximate depths obtained from the reciprocal analyses. The cross-sections generated from the tomographic inversions showed contoured variations of shear wave velocity with depth. These models, in addition to the reciprocal analyses, overestimated the depth of the till by up to four metres. This result is consistent with a velocity inversion. Consequently, the depth of the upper boundary of the till in all of the cross-sections was scaled to correlate with the depths observed in the boreholes. One of these adjusted tomographic models is presented in Figure 6.

A comparison between the depths to till interpreted from the SR results and from the borehole data is not presented because of the effects of the scaling used to match the SR data to the boreholes. The necessity of this modification of the SR results in this inverse layering case identifies ERI as the better of the first two geophysical methods for locating the depth to till. The trends in the slope of the layers shown in the SR cross-sections do however correlate to the ERI cross-sections and the borehole data. The thickness of the top two layers predicted by the SR results did not correlate well with borehole data because the refraction resolution was not adequate to detect these thin layers (0.5 to 1.5 metres).

5.3 MASW

The surface wave results compared with the borehole data are presented in Table 2. A typical velocity profile generated from the MASW analysis is shown in Figure 7. MASW inversion was completed for each line using a commercial software package (SWAN, GeoStudy Astier, 2008). The MASW inversions provided layered models with average layer thicknesses and velocity values across each of the five survey lines. In general, the MASW cross-sections show all four distinct layers identified in the borehole investigation; a surficial layer with shear wave velocity ranging from 62 to 119 m/s, a second layer with shear wave velocity ranging from 320 to 423 m/s, a third layer with shear wave velocity ranging from 188 to 334 m/s, and finally a fourth layer with shear wave velocity ranging from 569 to 1266 m/s. These velocity values correlate well to the range of expected velocities for the materials identified by the boreholes. The MASW survey was the only geophysical method studied that clearly identified the inverse layering at all the survey lines.

Table 2 indicates that the MASW method delivered a consistent underestimation of the depth to the till by up to 3.3 m. The comparison of the average layer thicknesses across each survey line from the MASW method with the single-point thicknesses identified in the boreholes on or nearby the survey lines may contribute to this error. Furthermore, one of the limitations of the MASW method is decreased resolution in the definition of deeper layers if the generation of frequencies below 15 Hz at the source is limited. The drop-weight source used in this study generated low frequencies but they were not strong enough to have better resolution of the deeper layers. For future MASW tests the drop-weight source should be modified to enhance the generation of low frequencies.

Table 2: Layer thicknesses predicted by MASW

BH No. (MASW Line)	Layer	Layer Thickness (m) From BH	From MASW	Diff
08-1 (Line 2-1)	1	1.2	0.7	-0.5
	2	1.7	1.5	-0.2
	3	6.1	5.2	-0.9
	Till Depth	9.0	7.4	-1.6
08-3 (Line 2-3)	1	0.6	0.9	0.3
	2	1.7	2.0	0.3
	3	3.8	3.1	-0.7
	Till Depth	6.1	6.0	-0.1
08-4 (Line 2-2)	1	0.6	0.6	0.0
	2	1.5	1.4	-0.1
	3	8.6	5.4	-3.2
	Till Depth	10.7	7.4	-3.3
08-5 (Line 1-1)	1	1.3	1.4	0.1
	2	1.0	1.1	0.1
	3	3.8	1.6	-2.2
	Till Depth	n/a[1]	4.2	n/a[1]
08-6 (Line 1-1)	1	1.4	1.4	0.0
	2	1.3	1.1	-0.2
	3	1.9	1.6	-0.3
	Till Depth	4.6	4.2	-0.4
08-7 (Line 2-2)	1	0.5	0.6	0.1
	2	3.2	1.4	-1.8
	3	6.4	5.4	-1.0
	Till Depth	10.1	7.4	-2.7

[1]no comparison because till depth from BH08-5 is in buried creek bed

The MASW results predict the thicknesses of the upper three layers with varying degrees of accuracy. Again, some of this error may arise from comparing average values to discrete location measurements. The range in error generally increased with each successively deeper layer, further illustrating a decrease in resolution with depth.

6 CONCLUSIONS

Three geophysical methods were compared in their ability to accurately delineate stratigraphy at a test site: electric resistivity imaging, seismic refraction, and multiple-channel analysis of surface waves. The results were verified by drilling boreholes. The boreholes revealed three general layers overlying a glacial till across the site. In addition, a stiffness reversal with depth was observed between the second layer from the surface (compact sand and silt) and the layer overlying the till (soft silty clay).

The electrical resistivity results were best for determining the depth to the competent layer (till) which ranged from 4.6 and 10.7 m across the site. However the 4 m electrode spacing used was too wide to deliver sufficient resolution for the ERI survey to accurately

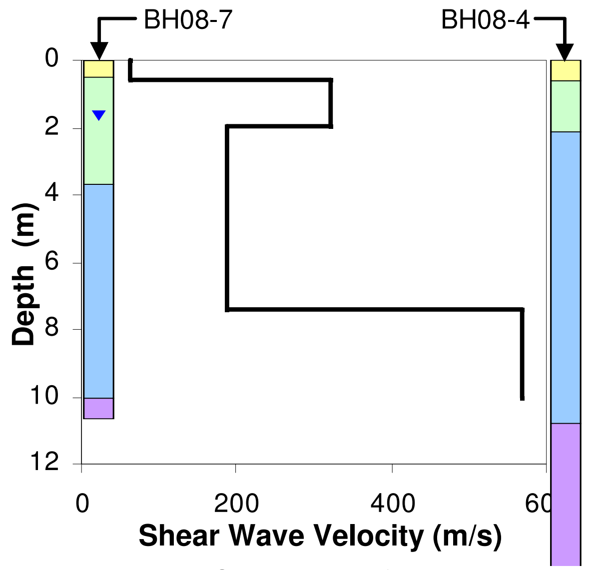

Figure 7. Typical MASW velocity profile (Line 2-2)

predict the vertical location of the overlying strata.

The SR results overestimated the depth of the till because of the presence of a stiff layer overlying a soft silty clay (i.e. velocity reversal).

The MASW results predicted the depth to till less accurately than the ERI. Using a source that generates higher energy in the lower frequency spectrum may help increase the depth resolution for this method. MASW was best able to detect the three distinct layers above the till (velocity reversal), even though the accuracy of predicted layer thicknesses varied across the site.

The complementary use of the three tested geophysical techniques was a successful approach in determining the main soil units and the depth of the competent layer (till) at the site because of the better characterization of the soil profile that is obtained by measuring mechanical and electrical soil properties. These methods have the potential to provide more accurate, and cost-effective subsurface modelling of the stratigraphy and the depth to a competent layer in soft overburden.

ACKNOWLEDGEMENTS

The authors would like to acknowledge the contribution of the Ministry of Transportation of Ontario (MTO) for the permission to perform the geophysical tests, Zahid Khan for the revision and evaluation of the results, Thurber Engineering Ltd. for the participation in the logistics and field support during the measurements, Geostudi Astier S.r.l. for the permission to use the program SWAN for the inversion of surface waves, and Fernando Tallavo, Yanjun Yang, Soheil Moayerian, Peter Pehme, and Chris Phillips for their help with the experimental program and data processing. Our gratitude also goes to Natural Sciences and Engineering Research Council of Canada (NSERC), OCE-Centre for Earth and Environmental Technologies, and Waterloo-Geophysics Inc. for the funding and in-kind contributions for this research.

REFERENCES

Ceverny, V., Langer, J., and Psencik, I. 1974. Computation of geometrical spreading of seismic body waves in laterally inhomogeneous media with curved interfaces. *Geophysical Journal of the Royal Astronomical Society*, 38(1): 9 - 19.

Griaff, K. 1991. *Wave motion in elastic solids*. Dover Publications, Inc., New York, NY, USA.

Hagedoorn, J. 1959. The plus-minus method of interpreting seismic refraction sections. *Geophysical Prospecting*, 7:158 - 182.

Keary, P., Brooks, M., and Hill, I. 2002. *An introduction to geophysical exploration*, 3rd ed., Blackwell Science Ltd., Malden, MA, USA.

Lai, C. G., and Wilmanski, K. (Eds.). 2005. *Surface waves in geomechanics: Direct and inverse modeling for soils and rocks.* CISM Courses and Lectures No. 481, International Centre for Mechanical Sciences.

McNeill, J. D., 1980. Electrical conductivity of soils and rocks. *Geonics Technical Note TN-5*, Geonics Limited, Mississauga.

Menke, W. 1989. Geophysical analysis: Discrete inverse theory. *International Geophysics Series*, Academic Press, San Diego, CA, USA. 289 pp.

Palmer, D. 1981. The generalized reciprocal method of seismic refraction interpretation. *Geophysics*, 46(11): 1508 - 1518.

Santamarina, J. C., Rinaldi, V. A., Fratta, D., Klein, K. A., Wang, Y.-H., Cho, G.-C., and Cascante, G. 2005. A survey of elastic and electromagnetic properties of near-surface soils. *Near-Surface Geophysics*, Ed. D. Buttler, SEG, Tulsa, OK, USA. pp. 71-87.

Stokoe II, K. H., and Nazatian, S. 1983. Effectiveness of ground improvement from spectral analysys of surface waves. In Proceedings of the *8th European conference on Soil Mechanics and Foundation Engineering*: Improvement of Ground, Rathmayer, H. G., and Saari, K. H. O. (eds), Helsinki, Finland. Pp. 91 - 94.